Thermal Conductivity Measurements of Graphite Samples

Amanda Noranzyk
Office of Science, Science Undergraduate Laboratory Internship Program
Correspondence: anoranzy@mines.edu

Colorado School of Mines
Golden, CO 80401

Los Alamos National Laboratory
Los Alamos, New Mexico 87545

August 12, 2009

Prepared in partial fulfillment of the requirement of the Office of Science, Department of Energy's Science Undergraduate Laboratory Internship under the direction of Dr. Todd A. Jankowski in the Applied Engineering Technology (AET) division at Los Alamos National Laboratory.

TABLE OF CONTENTS

FIGURES

Abstract

All materials have a property of thermal conductivity (k). As a measure of ability to conduct heat energy, k is a valuable number in heat transfer design and analysis. Knowing a material's value of thermal conductivity allows for proper selection in its use. The Applied Engineering Technology group at Los Alamos National Laboratory wishes to measure the thermal conductivity of various solid samples with minimal error. An apparatus was built in an attempt to measure a large range and variety of samples using a method combined from ASTM standards and the writer's ideas. The sample was heated on one end and cooled on the other. The temperature distribution across the sample was measured and a value of k calculated. Using Fourier's Law the results of the one material tested, graphite, produced a k value of 129.16 ± 4.69 W/mK the first time, 126.63 ± 2.90 W/mK the next and 127.31 ± 2.27 W/mK in the final run. The expected result based on the manufacturer's data sheet was 130 W/mK. The apparatus can now be used to measure various samples. Additionally, methods have been developed to estimate the errors associated with each new measurement.

1. Introduction

The science of heat transfer not only attempts to explain how heat energy may be transferred but is also used to predict the rate at which it will be transferred at certain specified conditions. Key elements in determining heat transfer include: a sample cross-sectional area, sample length, change in temperature across the sample, and a value of thermal conductivity. As one of the most meaningful values, thermal conductivity is a measure of how well heat energy travels through a material. Materials with lower values of thermal conductivity, k, such as silica, air, or wood, are considered insulators, as higher values of k, such as diamond, silver, and copper are conductors [1].

A number of methods have been developed and used to measure the thermal conductivity of various materials. Most of these methods have a limit on accuracy based on a range of temperatures and a sample's thermal conductivity. There is currently no single apparatus to measure all ranges of temperatures, thermal conductivities, or sample sizes. Standards such as ASTM E1225-04 [2] have been the closest in measuring large ranges of conductivity as it has a range of $0.2<k<200$ W/mK, but also requires that the sample be known to have a thermal conductivity close to its meter bars; so for an unknown sample, results are not practical and lack accuracy. A more common method is a hot plate method such as standard, ASTM C177-04 [3]. A specimen is placed between a cold plate and a hot plate and using the change in temperature and Fourier's Law, a value for k can be found. However, this Hot Plate method is best for materials with low thermal conductivity, insulators, and lacks a large range for measuring various materials.

The biggest problem in measuring thermal conductivity in any of these methods is the error due to heat loss. Even when insulating the sample and/or apparatus it is unclear how much heat energy is lost to the surroundings through radiation and convection. The use of a vacuum minimizes these errors because the only heat loss is through radiation [4]. However, there is no way to eliminate the heat loss error completely.

In Section 2, the methods used to measure thermal conductivity are presented. Also in Section 2 are the equations necessary to estimate the error in measurements. In Section 3 these methods and equations are utilized to reproduce known sample thermal conductivity values and also used to determine thermal conductivity values of unknown samples. After results are presented, conclusions are drawn in Section 4.

2. Methods

$$\dot{Q} = \frac{dQ}{dt} = kA\frac{\Delta T}{x} \tag{1}$$

$$k = \frac{\dot{Q}x}{A\Delta T} \tag{2}$$

Fourier's Conduction Law which governs heat transfer, **Eq. (1)**, is rearranged to calculate the thermal conductivity, k, **Eq. (2)**. Both **Eqs. (1)** and **(2)** are used for one-dimensional heat transfer. The goal of this project is to design an apparatus to approximate this one-dimensional heat transfer through a sample to determine its thermal conductivity value with minimal error.

2.1 Error Analysis

Anytime a measurement is made there is always an uncertainty which leads to error in the final calculation. When combining multiple measurements into an equation to calculate another value an overall error estimation on the final answer must be made when combining the errors from each element of the equation. In the measurement of thermal conductivity the total error propagates from various sources including error associated with the measurement of temperature, length, area, and heat transfer rate. Together the errors all contribute to the uncertainty in k.

For accurate measurements this total error needs to be calculated and minimized. The error is calculated using the Kline-McClintock Second Power Law [4]. This law can be explained using a simple equation such as Z=X*Y. For example say in the lab X is determined to be 4.71 with an uncertainty of ± 0.02 and Y to be 6.32 with an uncertainty of ± 0.50. Knowing this an overall uncertainty in Z can be calculated as follows:

$$U_Z = \sqrt{\left(\left(\frac{dZ}{dX}\right)(U_X)\right)^2 + \left(\left(\frac{dZ}{dY}\right)(U_Y)\right)^2} \tag{3}$$

$$U_Z = \sqrt{\left((Y)(U_X)\right)^2 + \left((X)(U_Y)\right)^2} \tag{4}$$

$$U_Z = \sqrt{\left((6.32)(0.02)\right)^2 + \left((4.71)(0.50)\right)^2} \tag{5}$$

$U_Z = 2.36$. Therefore using the Kline-McClintock Second Power Law the correct way to represent Z with error is: 29.77 ± 2.36 units.

2.1.1 Error Associated with Sample Length (dial caliper)

The dial caliper can measure to 0.001" and one can assume error to half of the next decimal place, 0.0005". This error is taken into consideration for both the length of the sample as well as in calculating its cross-sectional area.

2.1.2 Error Associated with Sample Cross-Sectional Area (A=pi*d^2/4)

The uncertainty in measuring the diameter will propagate in uncertainty in the cross-sectional area through the equation $A = \left(\pi d^2\right)/4$. The Kline-McClintock Second Power Law is used again and the error in calculated cross sectional area is equal to $U_A = \pm\sqrt{\left(\left(0.5\pi d\right)\left(U_d\right)\right)^2}$.

2.1.3 Uncertainty in Heat Load Through Sample (heat loss)

$$U_{\dot{Q}} = \left\{ \begin{matrix} \varepsilon\sigma F A_S (T^4 - T_S^4) & \text{un-insulated} \\ k_{MLI} A_S \dfrac{(T - T_S)}{t_{MLI}} & \text{insulated} \end{matrix} \right\} \tag{6}$$

Uncertainty in heat load is primarily through heat loss. The sample can be either insulated or un-insulated. To minimize radial heat transfer and closely approximate one-dimensional transfer, the sample can be wrapped in multi-layer insulation (MLI) and placed in a vacuum chamber. For the un-insulated sample the amount of heat loss can be calculated by the Stefan Boltzmann Law, **Eq. (6) un-insulated**. As a conservative assumption, throughout the calculations, a surface emissivity of 1 and a view factor of 1 are assumed; as this will give the highest possible value of heat loss and will maximize the uncertainty associated with heat loss. For the insulated sample the heat loss is calculated from Fourier's Law, **Eq. (6) insulated**. In the equation for insulated sample we assume $k_{MLI} = 4x10^{-5} W/mK$, and t_{MLI} is the thickness of the MLI insulation layers[5]. In this case A_S is the exposed surface of the sample $A_S = \pi dL$.

2.1.4 Uncertainty in Temperature Difference (thermocouples)

$$\begin{aligned} U_{\Delta T} &= \sqrt{\left(\left(\frac{d\Delta T}{dT_1}\right)(U_{T_1})\right)^2 + \left(\left(\frac{d\Delta T}{dT_2}\right)(U_{T_2})\right)^2} \\ \Delta T &= (T_2 - T_1) \\ U_{T_1} &= U_{T_2} \\ U_{\Delta T} &= \sqrt{2} U_T \end{aligned} \tag{7}$$

Because the same thermocouples are used on either end of the sample the uncertainty in T_1 is equal to the uncertainty in T_2.

2.1.5 Uncertainty in Thermal Conductivity

Now with the uncertainties in $\dot{Q}$,A, L and ΔT, the uncertainty in k can be calculated.

$$U_k = \sqrt{\left(\left(\frac{dk}{d\dot{Q}}\right)(U_{\dot{Q}})\right)^2 + \left(\left(\frac{dk}{dx}\right)(U_x)\right)^2 + \left(\left(\frac{dk}{dA}\right)(U_A)\right)^2 + \left(\left(\frac{dk}{d\Delta T}\right)(U_{\Delta T})\right)^2} \tag{8}$$

Substituting **Eq. (2)** into **Eq. (8)** the uncertainty in k is calculated as follows:

$$U_k = \sqrt{\left(\left(\frac{x}{A\Delta T}\right)(U_{\dot{Q}})\right)^2 + \left(\left(\frac{\dot{Q}}{A\Delta T}\right)(U_x)\right)^2 + \left(\left(\frac{\dot{Q}x}{A^2\Delta T}\right)(U_A)\right)^2 + \left(\left(\frac{\dot{Q}x}{A\Delta T^2}\right)(U_{\Delta T})\right)^2} \tag{9}$$

Accurate temperature readings are significant in the overall uncertainty in k. Error in temperature measurements with a smaller difference in temperature across the sample affected the uncertainty in k the most. Type T thermocouples were selected because they are certified by the manufacturer for $\pm$ 0.50 °C. Plugging in values to **Eq. (9)** made it clear how subtle changes in the uncertainty in Q and T (the first and last terms of **Eq.(9)**) had the largest effect on the overall error.

2.1.6 Error Analysis Used to Select Power and Sample Geometry

In determining what sample geometry to use, various models were run using Solidworks simulation software to estimate temperatures in the sample. It was determined using a longer cylindrical sample would be most beneficial in creating a large change in temperature across the sample and also still fit in the existing vacuum chamber. ***Figure 1*** shows various lengths and powers simulated in Solidworks used to calculate error. ***Figure 2*** also shows an estimate of temperature distribution in the sample based on this simulation for the optimal sample of 12 inches length. At these various lengths and powers, it was determined that the best power to use with the hot plate would be 74.67 watts, the maximum power with one power source. With two power sources 190.62 watts may be reached, however the samples become high in temperature and more unsafe to handle or be combined with the MLI. Additionally, the error is not reduced significantly by increasing the power input beyond 75 W, again note ***Figure 1***.

2.1.7 Heating/Cooling Plates

Copper was chosen for the heating and cooling plates because of its high value of thermal conductance and its ability to effectively and evenly transfer heat to the samples. Copper is also a softer, easy to machine, material that would be less complicated to mill, as the cooling plate has been designed with a channel to run chilled water. Solidworks simulation was run on the hot plate to show uniform heat transfer just as a finite element analysis was run on the cold plate, using COMSOL, [6] to show the effectiveness of the channel in creating an isothermal boundary on the sample. ***See Figures 3, 4, and 5.***

2.1.8 Pump Curve – Cold Plate Design

$$\Delta P = \frac{1}{2}\rho V^2 f \frac{L}{D} \tag{10}$$

$$\Delta P = \rho g z \tag{11}$$

A basic flow test was performed on the Isotemp 1006 D water pump to calculate its pump curve. An operating point based on the pump curve and system curve then determines the flow rate of the cold plate. A ¼" diameter 132" long tube connected to the outlet of the pump was placed in a graduated cylinder at various heights to measure the time taken to fill 400ml of fluid. **Figure 6** shows the results of this experiment. A system curve was calculated from COMSOL. **Figure 7** shows a graph of the pump curve combined with the system curve the flow rate was determined to be 0.68 gpm. (The operating point is the point where the system and pump curves cross).

2.1.9 Heaters – Hot Plate Design

Ohmite wirewound resistors were chosen as a heat source to warm the hot plate end of the apparatus. Two 50 W 75Ω and one 50 W 50Ω resistors were chosen to run in a parallel circuit to produce the maximum wattage of power deliverable by the power supply. Limited by 50 volts (for safety considerations) these heaters produce a maximum heat load at 116.67 watts of power with one heat source and are simple to use while preventing out gassing in the vacuum chamber.

2.2 Thermal Contact Resistance

Generally it is nice to think when two smooth objects come in contact with one another that a perfect contact is made. However on the microscopic level no matter how smooth a surface may appear to the naked eye, the microscope shows peaks and valleys where actual, imperfect, thermal contact is made. The peaks make good material contact but the valleys form voids with air pockets. ***See Figure 8***. As mentioned before, air is a good insulator, and thus these pockets of air act as insulation. Fortunately, a property of thermal contact resistance can help calculate exactly how much temperature difference will exist across the contact region.

$$R_C = \frac{1}{h_C} = \frac{\Delta T}{\dot{Q} / A} \tag{12}$$

Thermal contact resistance, R_C, is calculated as in **Eq. (12).** Estimating the copper/graphite interface to be copper/aluminum, rearranging **Eq. (12)** gives a maximum temperature drop across the region of contact as 1.163 °C [7]. This equation is accurate for pressures in the range from 2 900 psi to 5 100 psi and the actual interface pressure will be 725 psi. (see below) Although the actual interface pressure is lower than the given pressures, the given pressures are considering milled materials whereas both the copper and graphite are polished.

2.3 Force/Torque Applied to Sample

Often times a grease or soft metal such as indium is used to help reduce the thermal contact resistance and increase contact between two surfaces. Because of the higher temperatures in this design, grease would induce out gassing in the vacuum chamber and indium foil sheets of the correct size are impractical by price. However an applied torque on the nuts will bring the apparatus tightly together and increase the contact pressure between the copper and sample, also increasing its thermal contact. Threaded rods were used to pull the apparatus together with eight ¼” nuts. Tightening of these nuts provides a better contact between the sample and copper plates to minimize the thermal contact resistance which could attribute error to the final calculation.

$$compression = \frac{F}{A} << 7250\,psi \tag{13}$$

Given the flexural strength of the graphite sample (7250psi) the compression strength is calculated in **Eq. (13).** This shows that the ratio of force per area must be much less than the flexural strength. With 10% of the considered strength and a 3 inch circular area the total allowable force is $5\,122.125\ \text{lb}_\text{f}$ or $1\,280.531\ \text{lb}_\text{f}$/rod

$$\tau = 0.2Fd \tag{14}$$

The torque is calculated with **Eq. (14)** [8] where F is the force allowed per rod calculated by **Eq. (13)**, and d is the nominal major diameter of the thread, (in this case 0.25inches) the maximum torque per nut to safely avoid breakage is $64.03\ \text{in-lb}_\text{f}$.

2.4 Assembly

The heat sink plate is composed of a ¼” and ½” thick 4” by 4” copper plate. The cooling channel is milled into the ¾” plate as according to ***Figure 9.*** A ½” fillet is applied to all four corners to avoid sharp points. Two holes are drilled for VCR fittings for the water input in the ¼” plate. Both plates have four equidistant holes drilled in ½” from the sides with a diameter of 0.281” to feed the threaded rods. The ¼” plate was placed over the milled out channel and attached with high temperature silver soldering to seal the water pathway. The final product of the cooling plate appears as a solid ¾” thick plate with four holes drilled through.

The heater plate is a ¾” solid copper plate identical to the coolant plate in shape. Four holes are dilled ½” from the edges with a diameter of 0.281” to line up with the holes in the coolant plate. On one side three wirewound resistors are attached so that an even amount of power distribution can be acquired and also allowing for parallel wiring without getting in the way of the rods or nuts. ***Figure 10*** shows the heater plate.

Both the copper plates and the graphite sample have small holes drilled for the thermocouples to be placed. ***Figure 11*** shows the location of each thermocouple. Position 4 is on the hot plate a ¼” from the contacting surface with the sample. Position 1 is ¼” from the hot end of the sample. Position 3 is located in the center of the sample. Position 2 is located ¼” from the edge of the sample on the cold end. Position 5 is on the copper cold plate ¼” from the contacting surface of the sample. All holes are drilled ½” deep into which the thermocouple resides.

A sample of length *x*, is placed between the two copper plates with the smooth sides against the sample. The threaded rods are fed through the holes in the copper plates and bolted on both ends and tightened to a total torque of 64.03 in-lb_f on each nut to increase contact between the materials. Five layers, 0.060 inches thick, of MLI wrap the entire apparatus with only holes for thermocouples, heater wires, and water feed-thrus to protrude. ***Figure 12*** shows the apparatus in the vacuum as simulated in Solidworks without MLI.

2.5 Data Collection Methods

Thermocouples attach to the sample and a HP 34970A Data Acquisition unit through a vacuum feed through. The unit, controlled by a computer, records temperature readings from the thermocouples on a given time interval set in the program, Agilent BenchLink Data Logger 3, v. 3.10.00. Steady-state temperatures are used in calculating k. ***Figure 13*** shows the apparatus prior to being wrapped in MLI, ***Figure 14*** shows the apparatus in the vacuum chamber with MLI, and ***Figure 15*** shows the entire experimental set-up.

3. Results and Discussion

Some preliminary tests were run with three inch long samples to test instrumentation. ***Figure 16*** shows the warming of the three inch sample with the cold plate temperature of 30 C. As a steady temperature is reached on both the hot and cold end of the sample a k value of 63.33 ± 3.16 W/mK is recorded. It is possible that that there was a large unaccounted for error since the 3 inch samples were not wrapped in MLI insulation. Additionally, the holes in the three inch long samples were only drilled ¼” deep into the sample leaving them close to the surface and radiating heat loss, possibly leading to such error. The samples were 20/20 grade graphite, isostatically pressed. The reported thermal conductivity from the manufacturer’s data sheet was 85 W/mK.

A 12 inch sample was ordered in a separate order and was to be of the same material in a longer length. The results however did not agree with the expected k value but were consistent through three runs at various power levels. For the 12 inch sample it took longer to reach a steady temperature as seen in ***Figure 17***, this is likely due to its increased length. The final thermocouples readings of one test are shown in ***Figure 18***, but note that the reading from location 3 seemed to have come loose from the sample and was not reading the sample temperature accurately. Excluding thermocouple 3 and using thermocouples 1 and 2, the calculated results are as follows: for the 42 W, 30 C, 12 inch test a k value of 129.16 ± 4.69 W/mK was calculated. For the 74.67 W, 30 C, 12 inch test a k value of 126.63 ± 2.90 /mK was measured. The 116.67 W, 30 C, 12 inch test had a k value of 127.31 ± 2.27 /mK. As shown in

Figure 19 the average k value is 127.7 W/mK which suggests that the 12 inch sample is a different composition of graphite. Going back to the company literature it was determined that another method of manufacturing called extruded had a different thermal conductivity than pressed graphite. At 130 W/mK this fine grain extruded graphite is likely what was shipped by mistake.

4. Summary and Conclusion

In conclusion, the results were consistent within the various temperature and voltage changes. It was determined after much experimentation and research that a different sample was sent than what was ordered. The results also show that the accuracy of the apparatus is within less than 5% depending on sample length.

During the multiple tests it was concluded that some parts of the apparatus could have been designed better. Getting the apparatus into the chamber was rather difficult for a single person to accomplish. Because the feedthrus in the door were too short to protrude all the way through, the water lines had to be connected to the door first rather than the apparatus. The apparatus then had to be connected to the door prior to insertion into the vacuum chamber. A solution to this may have been to make the chamber door removable as more a part of the apparatus itself. Then the thermocouples, water lines, and power connections could all be made at once and then simply slid into the chamber. Another solution would be to have more flexible hosing for the water feedthru, as the metal lines tend to twist up and push the apparatus further into the chamber than necessary.

For future work with this apparatus, the above changes are recommended before potential tests. This apparatus could be used to measure the difference in thermal conductivity between a coated and non-coated sample or simply to measure various sample types. This apparatus was intended to measure specific samples of graphite but was designed to measure a large range of materials. A ‘user friendly” version of the error approximation software was also developed in this process so that testing can continue without me.

5. Acknowledgements

Funding for this work was provided by Los Alamos National Laboratory (LANL), the Department of Energy (DOE) and the Offices of Science, Science Undergraduate Laboratory Internship (SULI). Los Alamos National Laboratory is operated by Los Alamos National Security LLC for the Department of Energy. The author thanks Dr. Todd Jankowski for his assistance.

6. References

1. Cengel, Y.A., *Heat Transfer A Practical Approach*. 1998, New York: McGraw-Hill. 1-202.
2. ASTM, *Thermal Conductivity of Solids by Means of the Guarded-Comparative-Longitudinal Heat Flow Technique*. 2004, ASTM International: West Conshohocken, PA. p. 1-8.
3. ASTM, *Steady-State Heat Flux Measuremnets and Thermal Transmission Properties by Means of the Guarded-Hot-Plate Apparatus*. 2004, ASTM international: West Conshohocken, PA. p. 1-22.
4. Beasley, D.E. and R.S. Figliola, *Uncertainty Analysis*, in *Theory and Design for Mechanical Measurements*. 1995, Joh Wiley & Sons, Inc.: New York. p. 171-200.
5. Flynn, T.M. and K.D. Timmerhaus, *Cryogenic Process Engineering*. The International Cryogenics Monograph Series. 1989, New York: Plenum Press.
6. *Comsol Multiphysics*: Los Angeles, California.
7. Holman, J.P., *Heat Transfer*, ed. 9. 2002, New York: McGraw-Hill.
8. Juvinall, R.C. and K.M. Marshek, *Fundamentals of Machine Component Design*. 2 ed. 1983, New York: John Wiley and Sons, Inc. . 339-342.

Nomenclature

A_C	Cross sectional area	ΔP	Change in Pressure
A_S	Surface Area	$\dot{Q}$	Heat Load
ε	Emissivity	R_C	Thermal Contact Resistance
D	Diameter	ρ	Density of Water
F	Force	σ	Stefan Boltzmann Constant
F	View Factor	T	Temperature
f	Flow Rate	T_S	Surrounding Temperature
h_C	Thermal Contact Conductance	ΔT	Change in Temperature
k	Thermal Conductivity	t_{MLI}	Thickness of MLI layering
L	Length of Tubing	x	Distance from one thermocouple to another

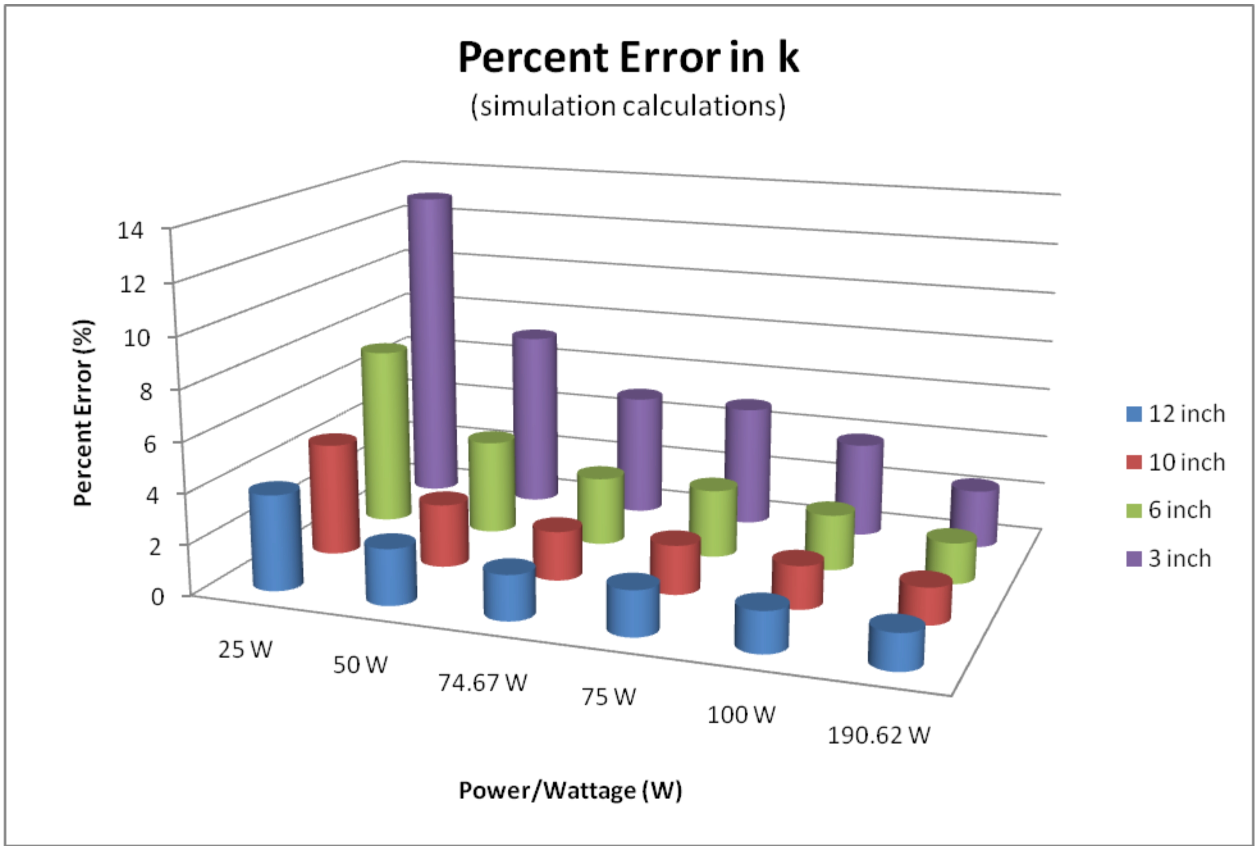

FIGURE 1. Graph of error calculation in the value of thermal conductivity. Sample with MLI insulation. The results show a longer sample and higher power input is best for best accuracy. Changes in temperature for the calculation were produced by Solidworks Simulation software 2009.

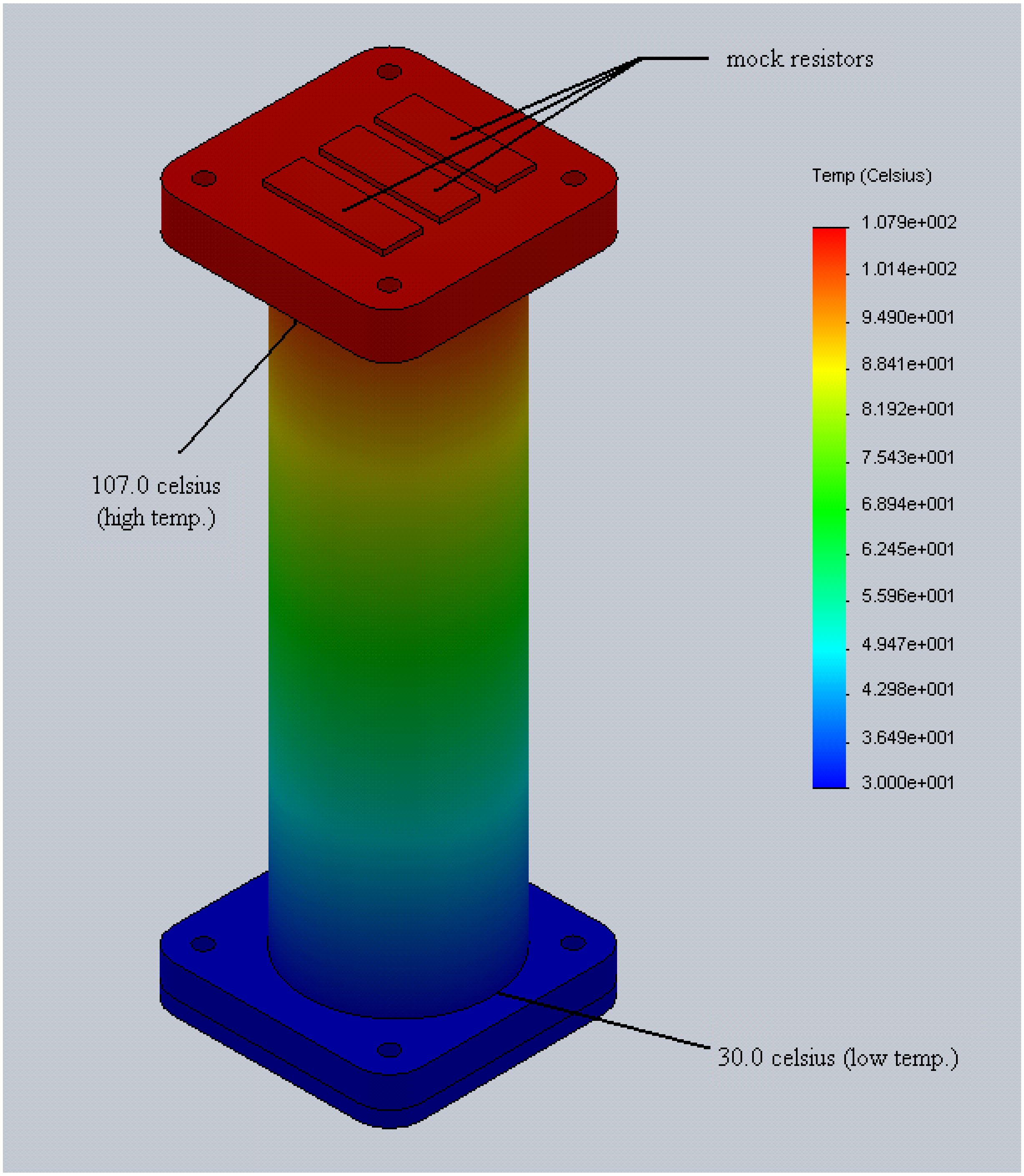

FIGURE 2. Estimate of temperature distribution based on an approximated 85.0 W/mK thermal conductivity in the sample. A 12 inch sample is run at 116.67 W. Mock apparatus set-up and temperatures provided by Solidworks Simulation add-on. Sample is without MLI insulation.

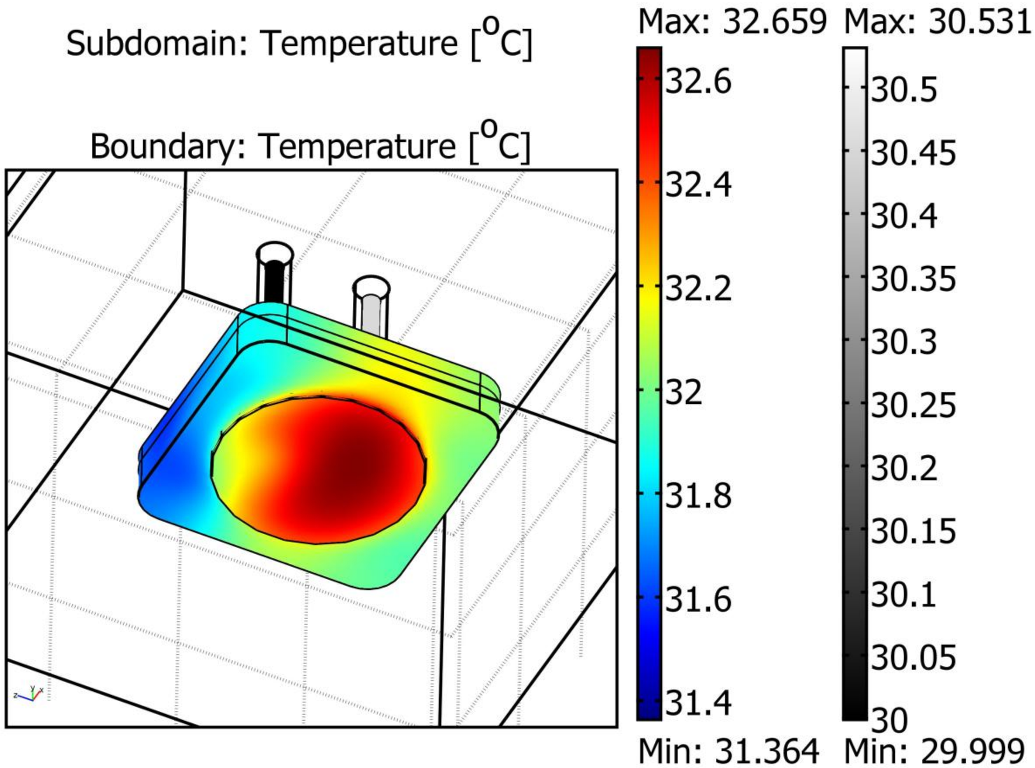

FIGURE 3. Cold plate testing in COMSOL. The maximum heat load is applied directly to the bottom surface. The inlet water temperature is set to 30 C with a flow rate of 0.68 gpm. The results show a fairly uniform temperature distribution in the copper, with a maximum of ~1C temperature difference between the hottest and coldest points.

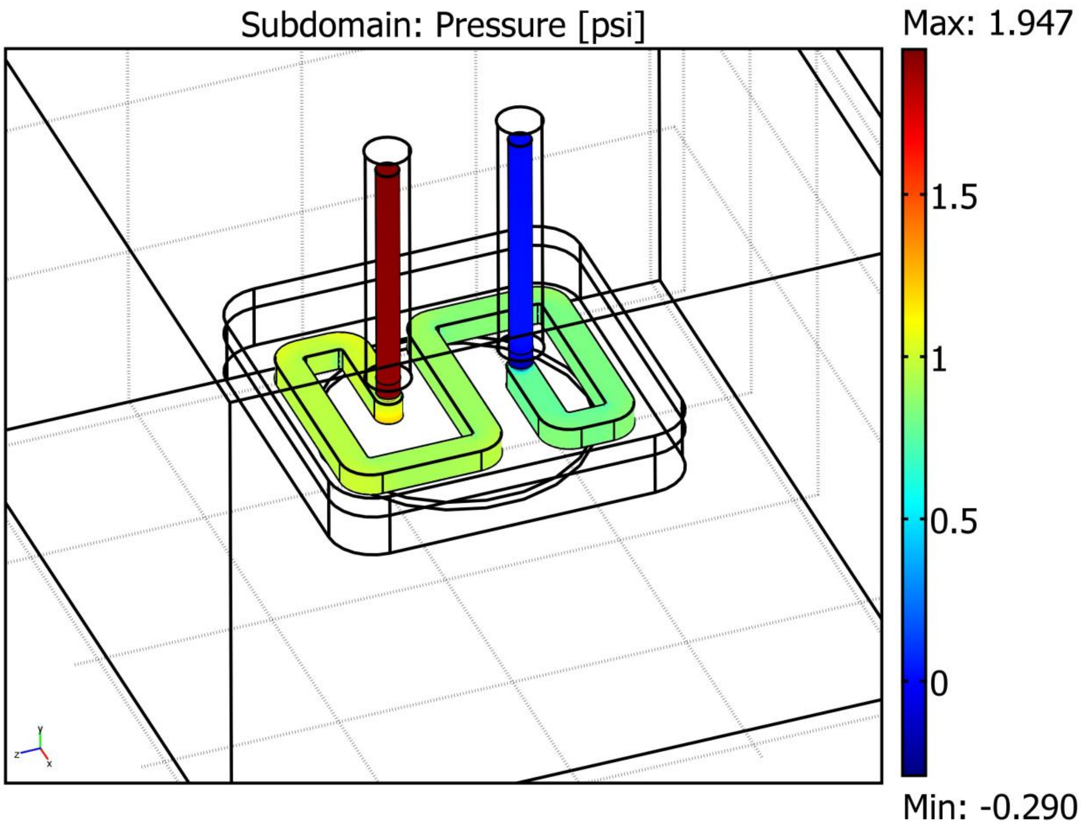

FIGURE 4. Pressures in the copper cooling plate channels.

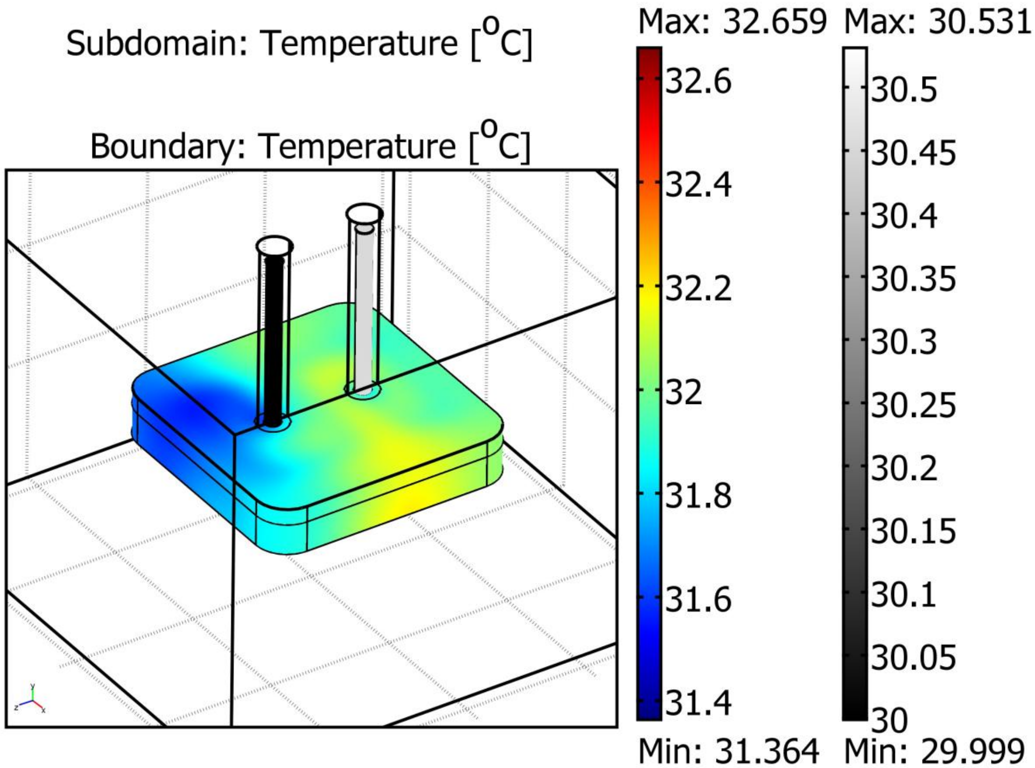

FIGURE 5. Temperature distribution across the cold plate, top view. The results show a maximum of ~1C temperature difference between the hottest and coldest points.

0 inch test	
Volume (ml)	*Time (s)*
800	14.34
400	7.06
400	7.11

0 psi
89.17×10^{-2} gpm

31.5 inch test	
Volume (ml)	*Time (s)*
400	8.21
400	7.83
400	8.06

1.14 psi
78.95×10^{-2} gpm

54.5 inch test	
Volume (ml)	*Time (s)*
400	9.37
400	9.19
400	9.50

1.97 psi
67.81×10^{-2} gpm

80 inch test	
Volume (ml)	*Time (s)*
400	37.00
400	11.00
400	11.10

2.89 psi
57.37×10^{-2} gpm

FIGURE 6. Isotemp 1006D Pump curve test results.

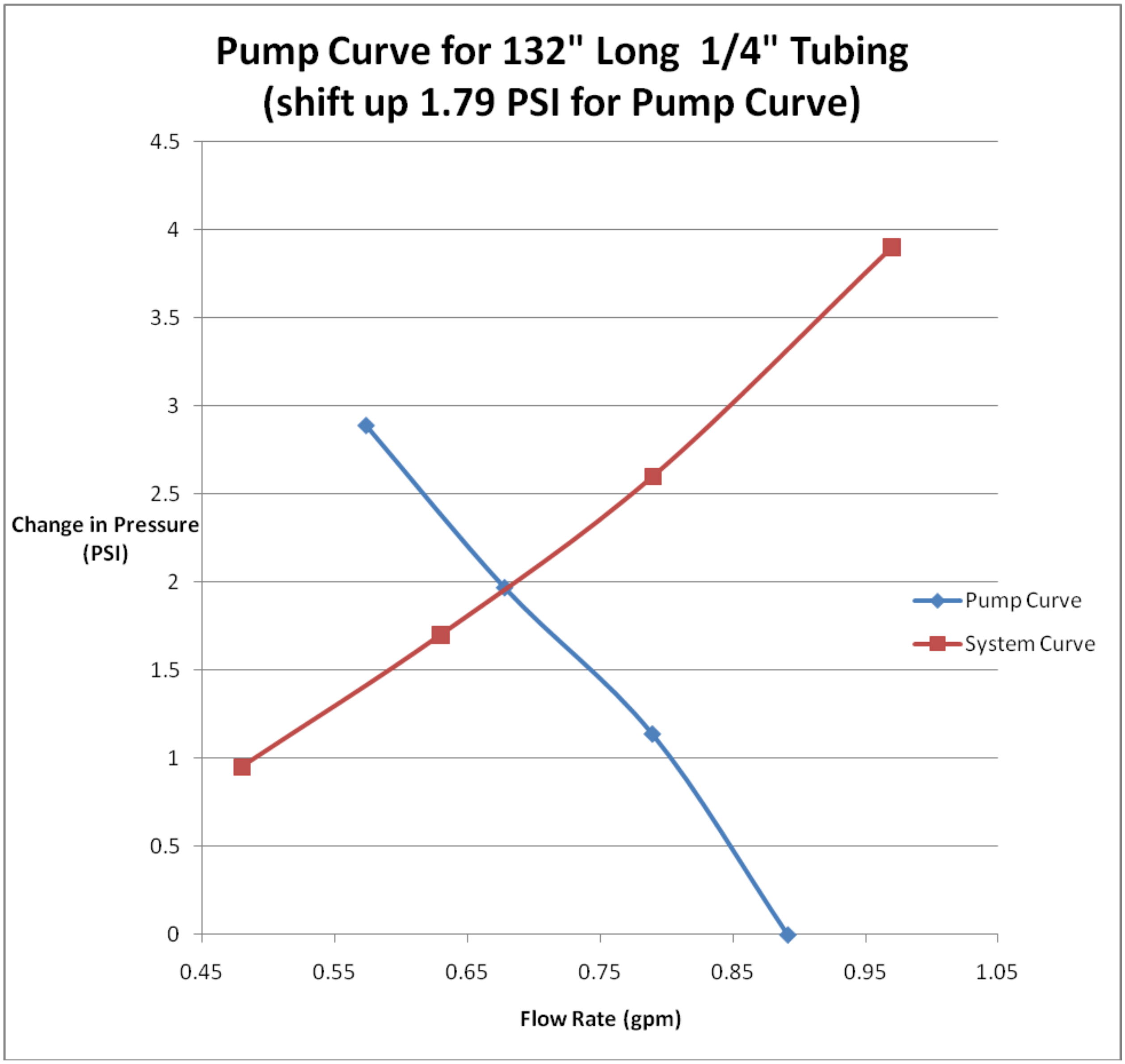

FIGURE 7. Operating point determined from a pump curve and a system curve on the Isotemp 1006D. Flow rate determined to be 0.68 gpm.

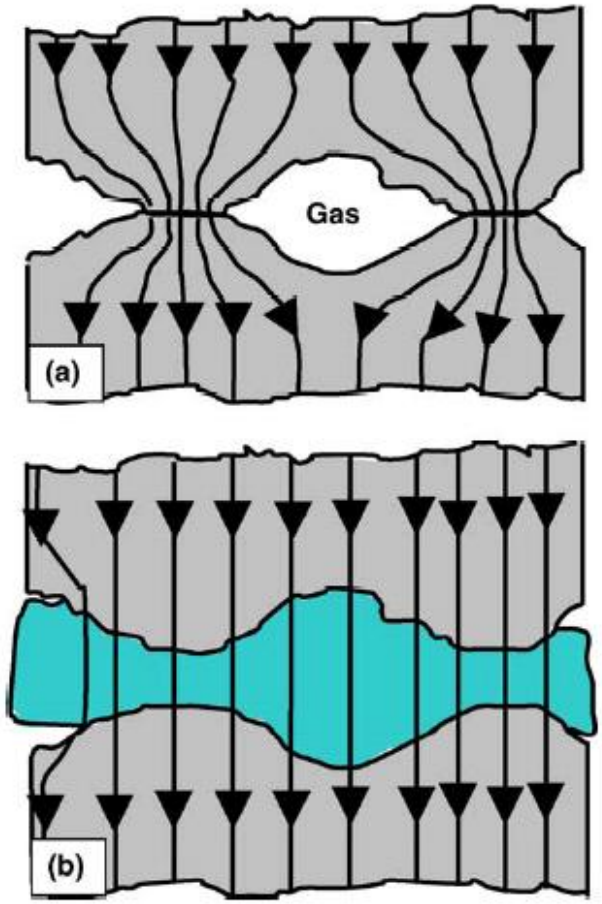

FIGURE 8. Illustration of thermal contact resistance. (a) Actual imperfect thermal contact (b) Ideal/perfect thermal contact, aided by a grease or soft metal realigning the distribution of heat energy. (http://www.ces.clemson.edu/~mica/Publications/Ref_132.pdf)

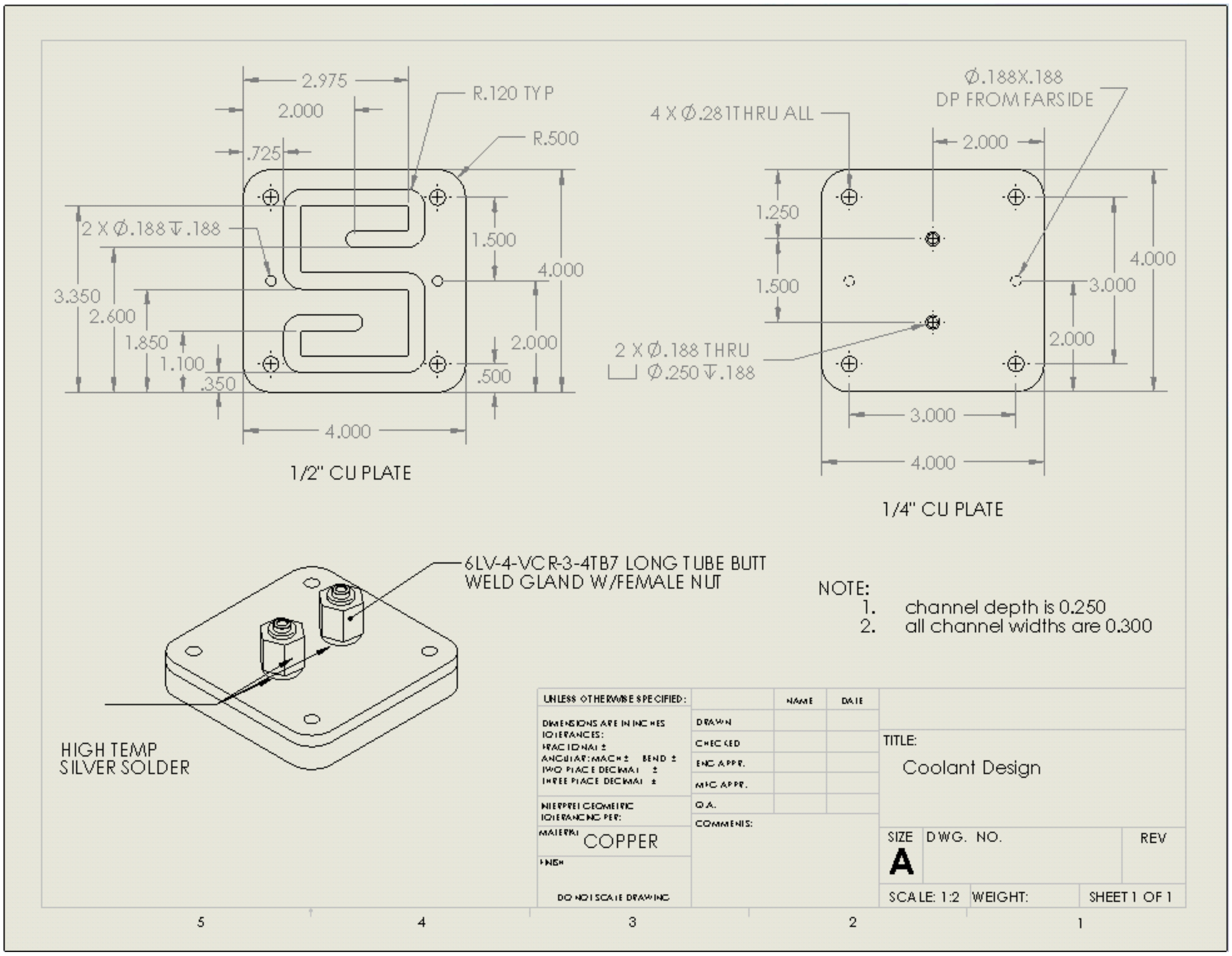

FIGURE 9. Cooling plate drawings for machine shop. Produced with Solidworks.

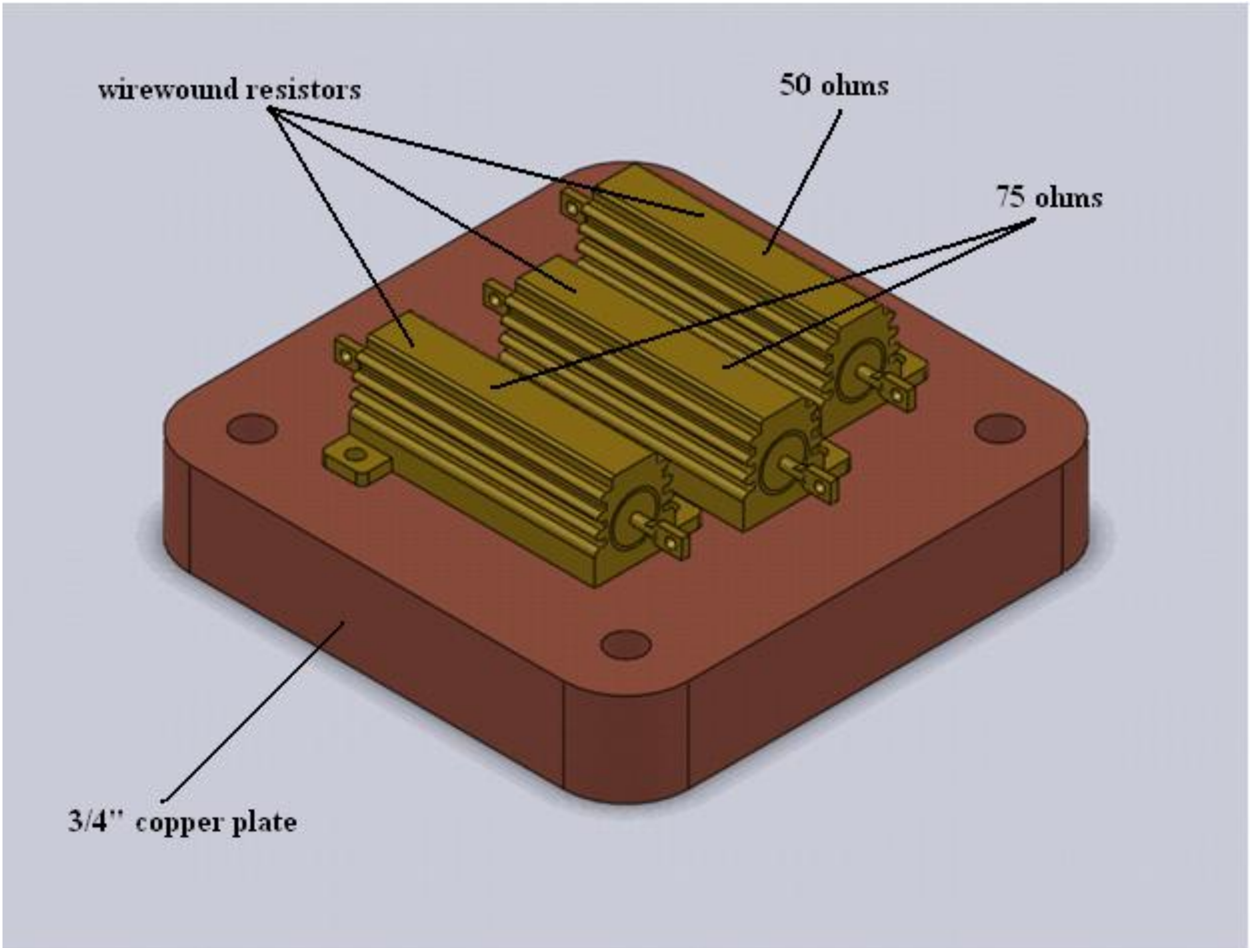

FIGURE 10. Heater Plate with wire wound heaters attached. Produced with Solidworks.

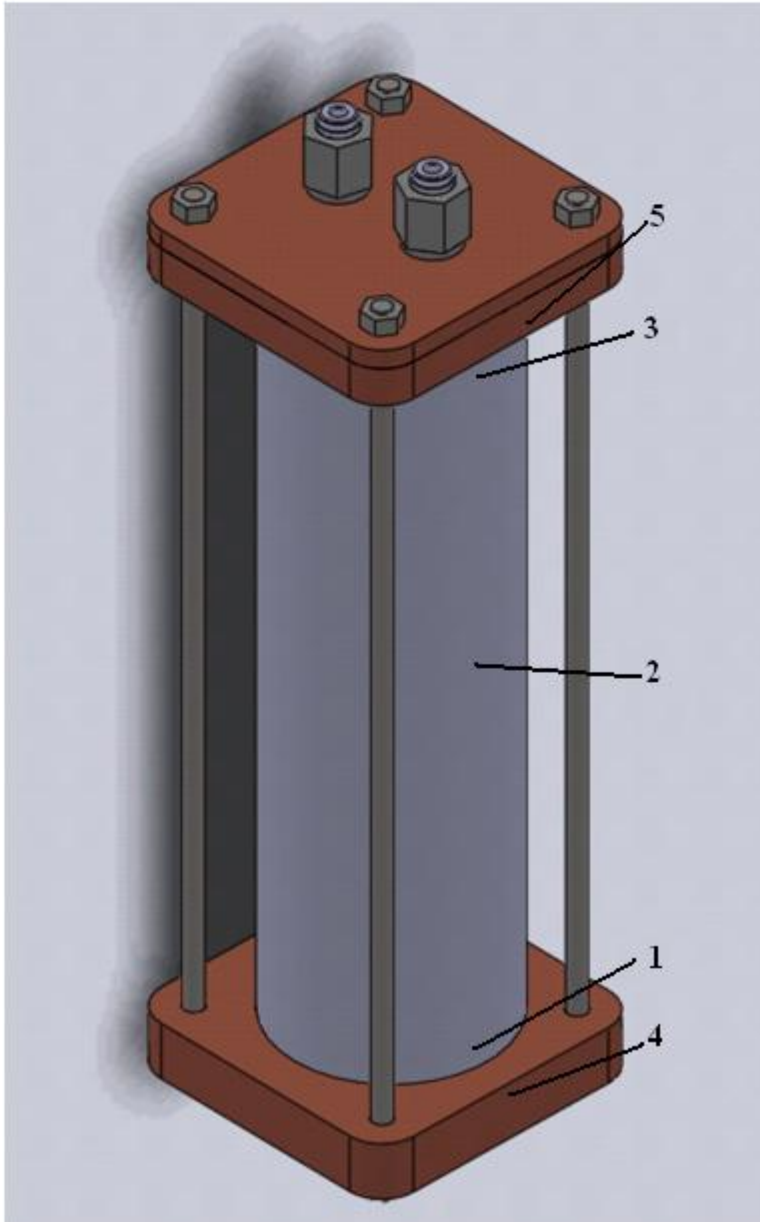

FIGURE 11. Thermocouple placement. 5 is on the copper cold plate ¼" from the contacting side with the sample. 3 is a ¼" into the sample from its edge. 2 is exactly the middle of the sample. 1 is a ¼" into the sample from its edge. 4 is on the hot plate ¼" from the contacting side with the sample. All holes are drilled ½" deep and the thermocouple is placed all the way in.

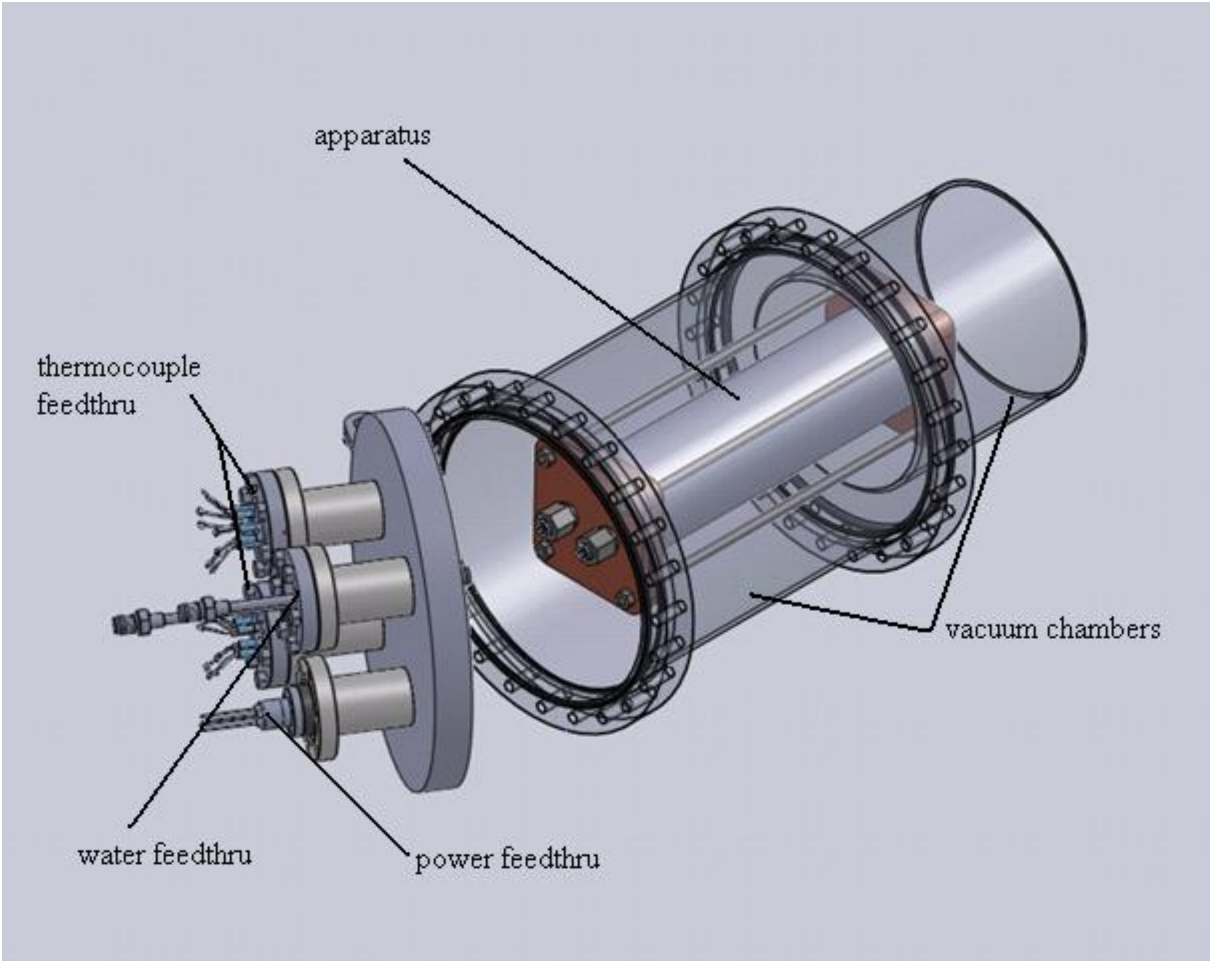

FIGURE 12. Apparatus inside vacuum chamber. Four ports were welded into the chamber door to allow thermocouples, resistor wires, and water tubes to pass between atmosphere and chamber so everything could be monitored and changed from the outside.

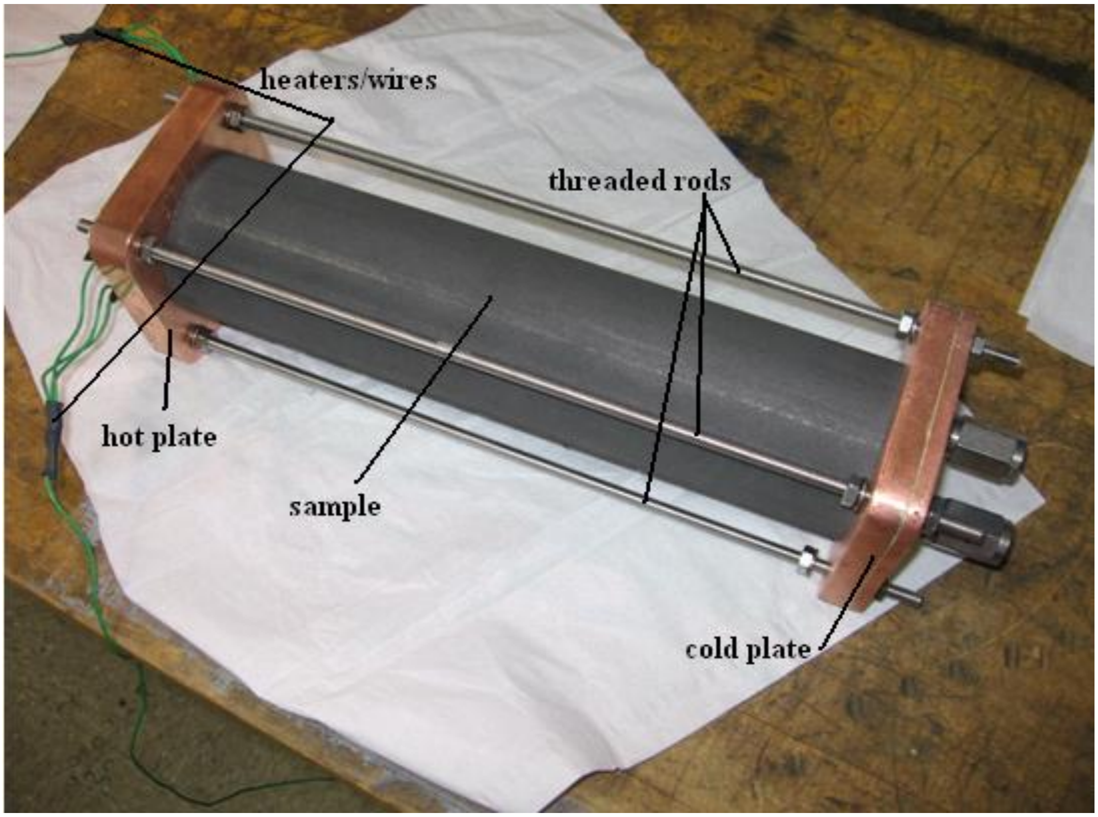

FIGURE 13. Assembled apparatus with 12 inch sample prior to being wrapped in MLI insulation.

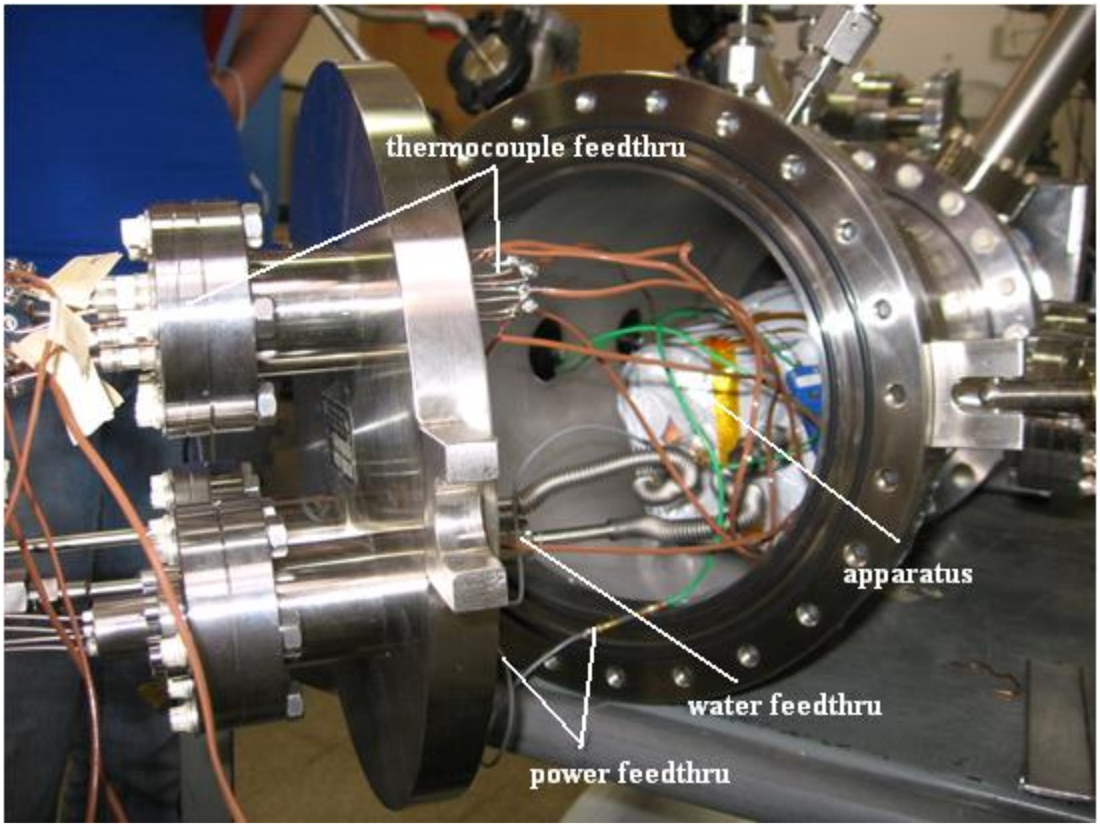

FIGURE 14. Complete assembly prior to closing vacuum door. Apparatus is wrapped in 5 layers of MLI insulation and all thermocouples, power wires, and water lines are connected. Vacuum is to reach 1.5 x 10^{-5} with this sample.

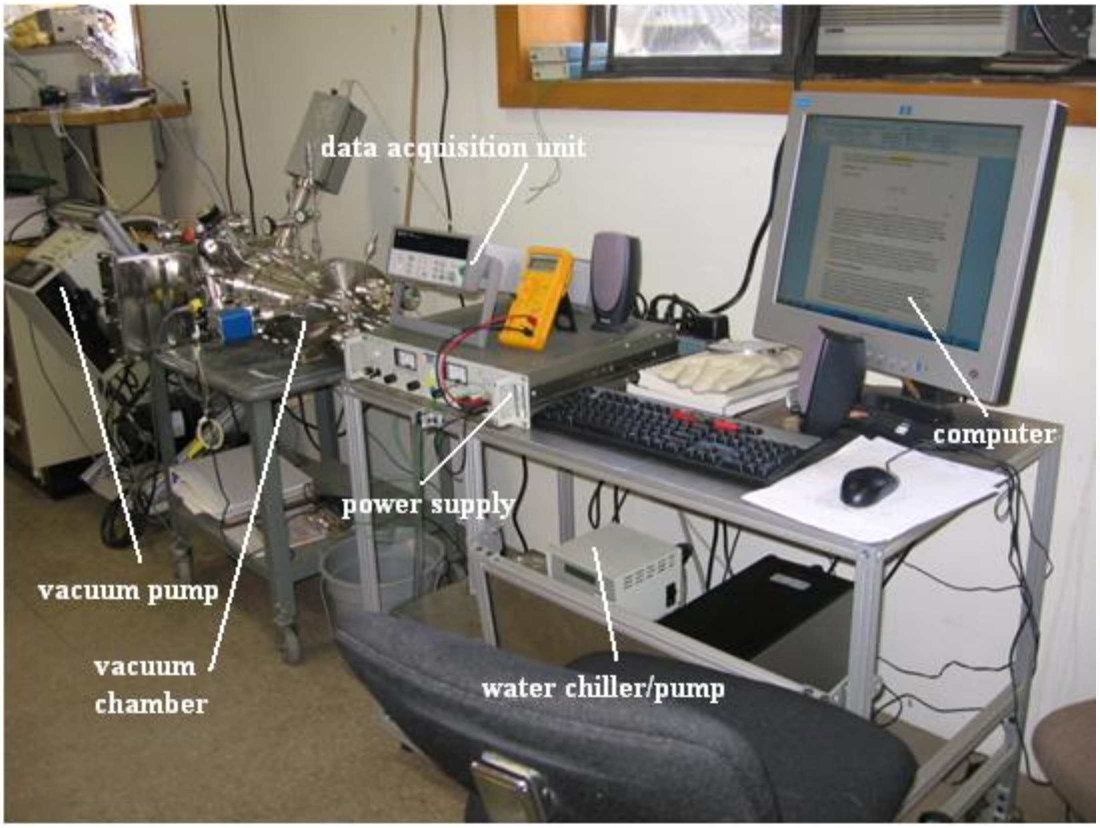

FIGURE 15. Complete testing set up.

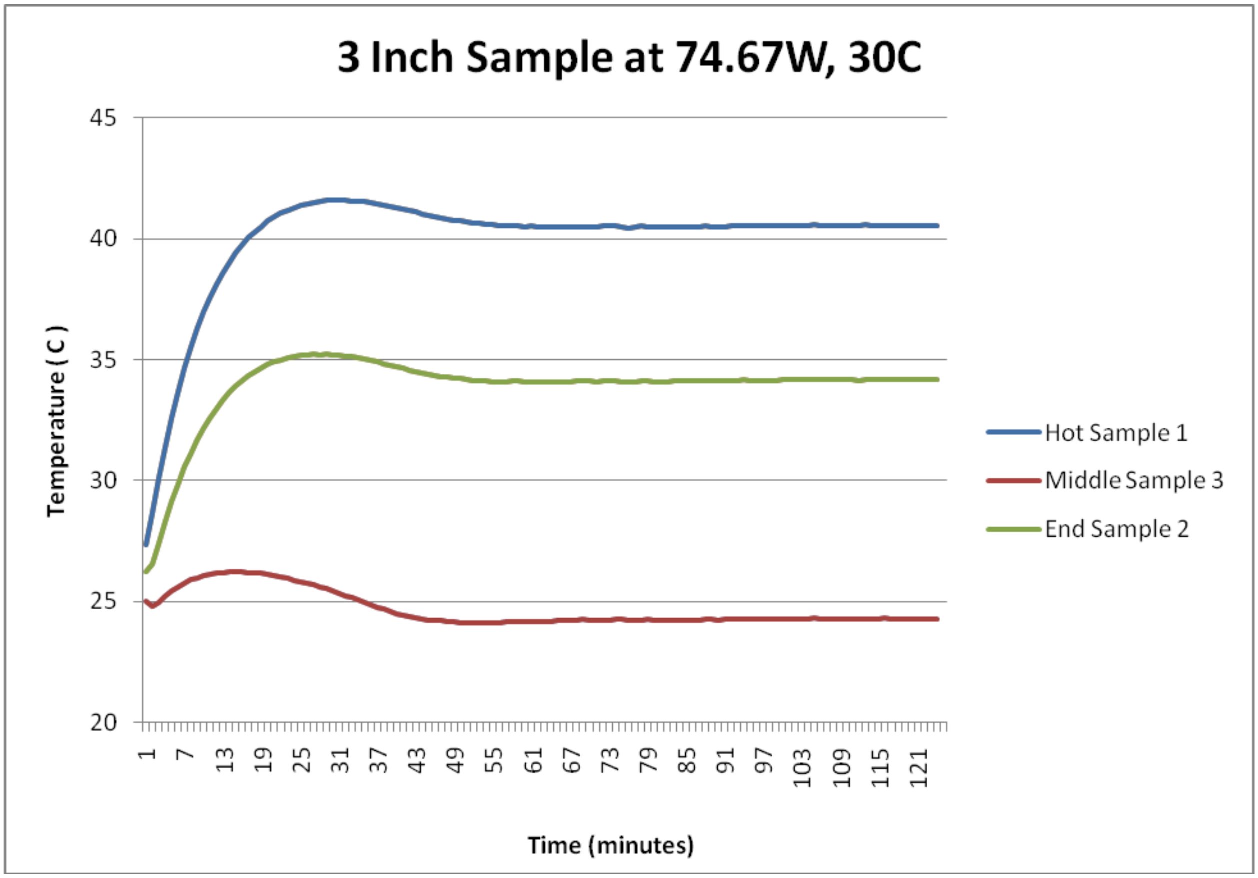

FIGURE 16. Data collection shows k=63.78 ± 2.93. Sample is without MLI insulation. Also, stick on thermocouples were used to measure the copper plate temperatures in the three inch sample, the data collected was invalid and therefore not presented. Holes were drilled for thermocouples and future testing.

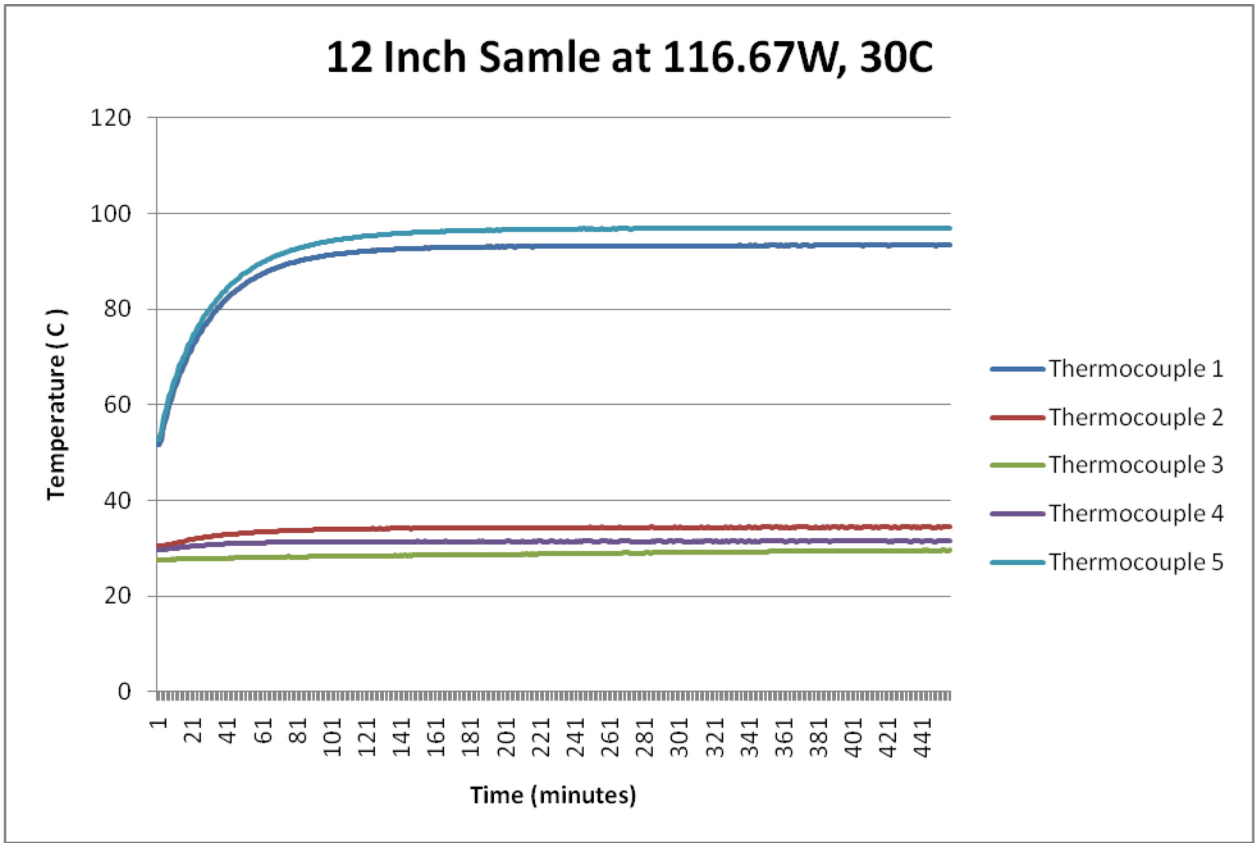

FIGURE 17. 12 inch sample at 116.67W, 30C coming up to steady temperature. Graph shows readings of all 5 thermocouples. It is clear that thermocouple 3 had dislocation with the sample as the results are not consistent with expectations.

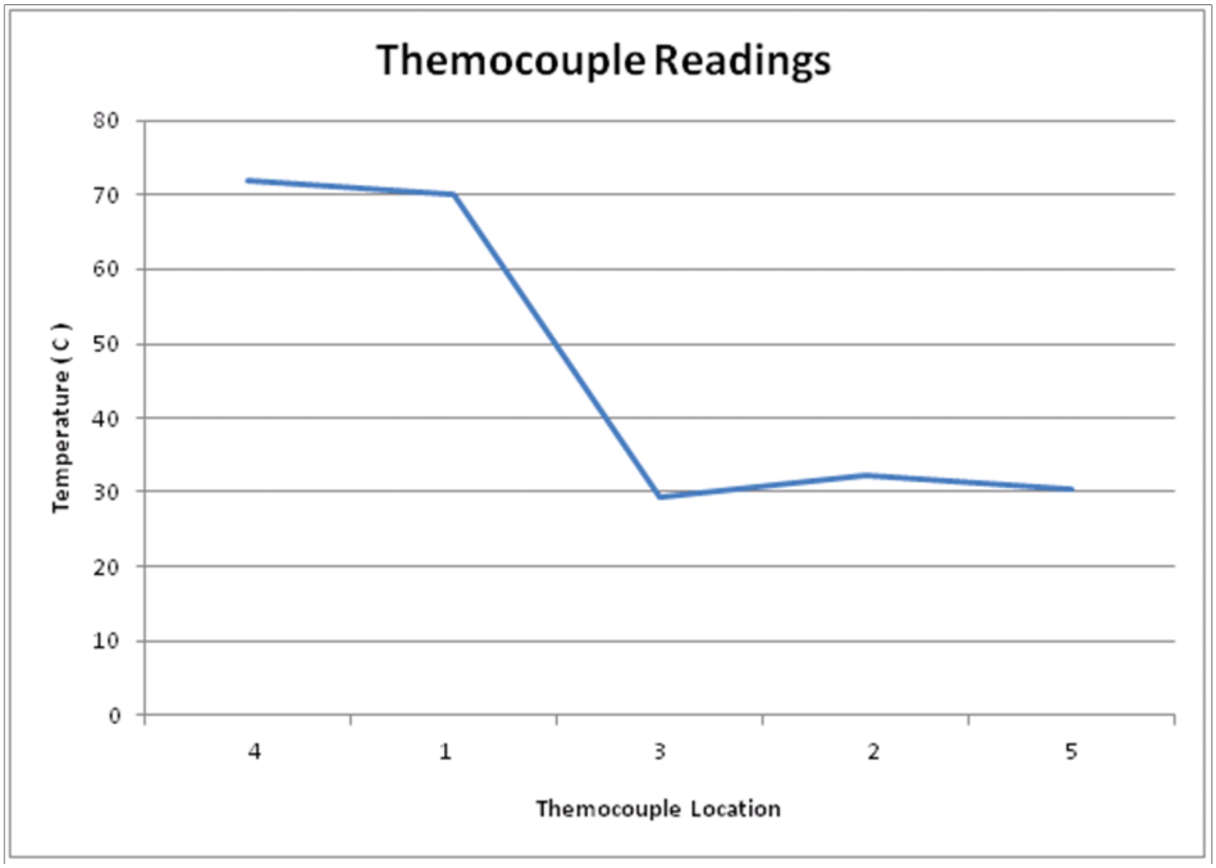

FIGURE 18. Final reading from thermocouples in 40V 30C test. A linear fit should be found but it is apparent that the thermocouple in location 3 was either lose or having error.

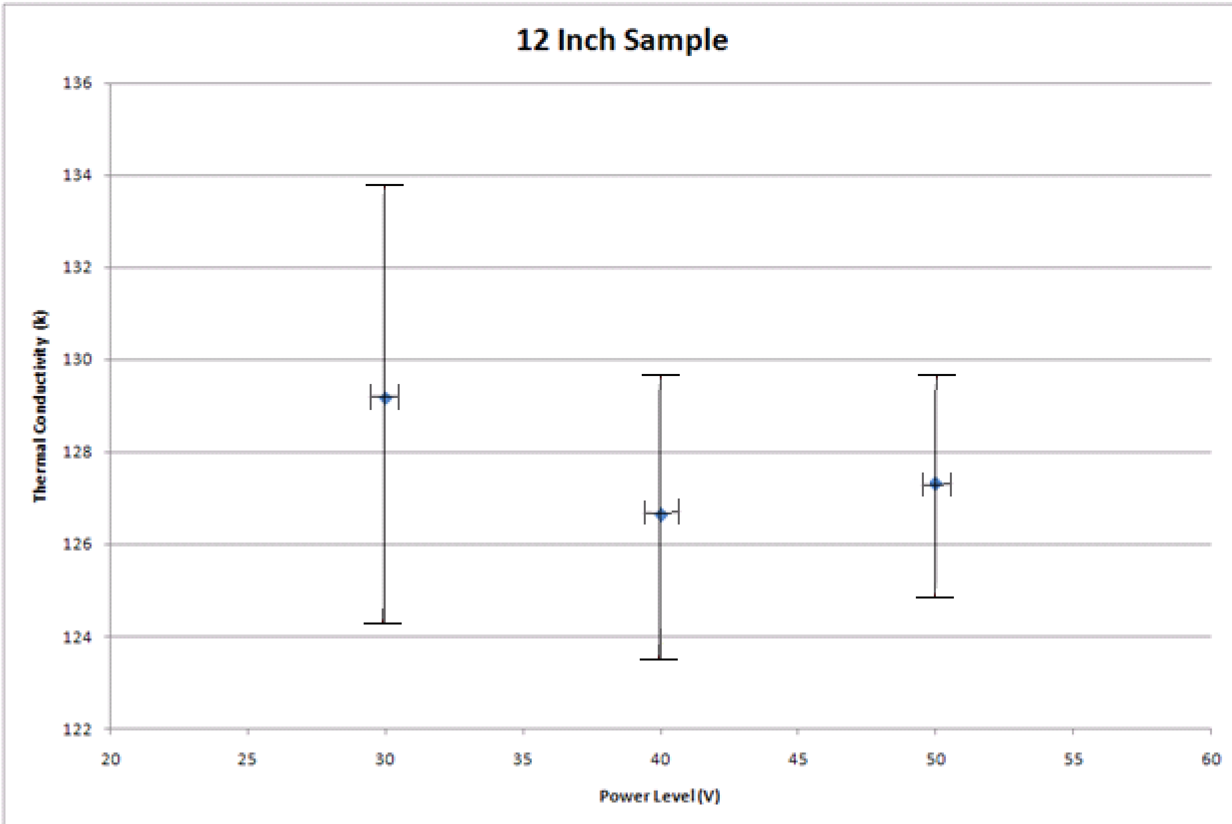

FIGURE 19. 12 inch sample at various power levels. Results show an average k =127.7 W/mK.